Active Flow Control in Supersonic Nozzles

Active flow control in supersonic nozzles

Michele Ferlauto

Citation: AIP Conference Proceedings **1978**, 470035 (2018); doi: 10.1063/1.5044105
View online: https://doi.org/10.1063/1.5044105
View Table of Contents: http://aip.scitation.org/toc/apc/1978/1
Published by the American Institute of Physics

Active Flow Control in Supersonic Nozzles

Michele Ferlauto[1,a)]

[1]*Department of Mechanical and Aerospace Engineering, Politecnico di Torino, Turin, Italy*

[a)]Corresponding author: michele.ferlauto@polito.it
URL: http://staff.polito.it/michele.ferlauto

Abstract. Active flow control in supersonic nozzle mainly concerns Fluidic Thrust Vectoring (FTV) strategies. Thrust Vectoring in fixed symmetric nozzles can be obtained by generating a local perturbation at wall causing flow separations, asymmetric pressure distributions and therefore, the vectoring of the primary jet thrust. The control action can be steady, e.g. continuous blowing, or pulsating, e.g. by synthetic jet actuators. In the paper a numerical procedure is explained, which is able to deal with most of the FTV strategies as well as with continuous and pulsating flow excitation. The flow governing equations are solved according to a finite volume discretization of the compressible URANS equations. The effectiveness of different combinations of FTV strategies and flow actuations are presented. The numerical results obtained are compared with the experimental data found in the open literature.

INTRODUCTION

The main application of jet-vectoring to the Aerospace field is also known as 'thrust vectoring'. Actual multi-axis thrust vectoring technology is based on movable nozzles which allow unconventional maneuvers safely, even if the aircraft is in aerodynamic stalled conditions[1]. Thrust vectoring is beneficial in terms of maneuverability and effectiveness of aircraft controls. It helps the vehicle to meet take-off and landing requirements and it is a valuable control effector at low dynamic pressures, where traditional aerodynamic controls are less effective[2]. Fluidic Thrust Vectoring (FTV) retains the advantages of mechanical thrust vectoring without the need of the complex adjustable hardware of the variable geometry devices [3]. FTV strategies follow the principle of flow manipulation to obtain a lateral force on a nozzle of fixed geometry. In general, the effect is obtained by injecting into the nozzle a secondary flow of bleed air. The injected fluid interacts with the exhaust flow into the fixed nozzle and, by breaking the symmetry, it generates wall pressure distributions that give rise to a side component of the thrust vector. The key point for the fluidic approach is the identification of a manipulation technique that can gradually modulate the symmetry-breaking effect within an acceptable range of deterioration of the nozzle performances[4]. Several manipulation strategies have been investigated in literature, e.g. shock vector control, counter-flows, throat shifting and supersonic dual-throat nozzle[2]. The performances of these approaches has been measured in terms of control efficiency and thrust loss. All these methods require continuous blowing of secondary flow or other kind of air spillage/bleed. Flow manipulation approaches other than continuous blowing are under testing. For instance, one can induce forcing based on synthetic jets [5, 6] or plasma actuators [7]. For this purpouse, adequate numerical tools for the evaluation of steady and unsteday nozzle performance are the privilege mean of investigation[8, 9]

In present paper the application of synthetic-jet actuators to jet vectoring is investigated numerically with the aim of testing the manipulation effectiveness and to analyze the system sensitivity to different forcing actions. Unsteady CFD analyses can help in deriving the time-varying nozzle performances, in clarifying the role and interaction between various nonlinear phenomena, in assessing and testing the open/closed-loop control. This is even more stringent when fully unsteady manipulators are used (e.g. synthetic jet actuators). By varying the number, locations, forcing intensities, frequency and phase displacement of the SJ actuators the resulting vectoring effects is studied for two different FTV approaches (shock vector control and dual-throat nozzle).

International Conference of Numerical Analysis and Applied Mathematics (ICNAAM 2017)
AIP Conf. Proc. 1978, 470035-1–470035-4; https://doi.org/10.1063/1.5044105
Published by AIP Publishing. 978-0-7354-1690-1/$30.00

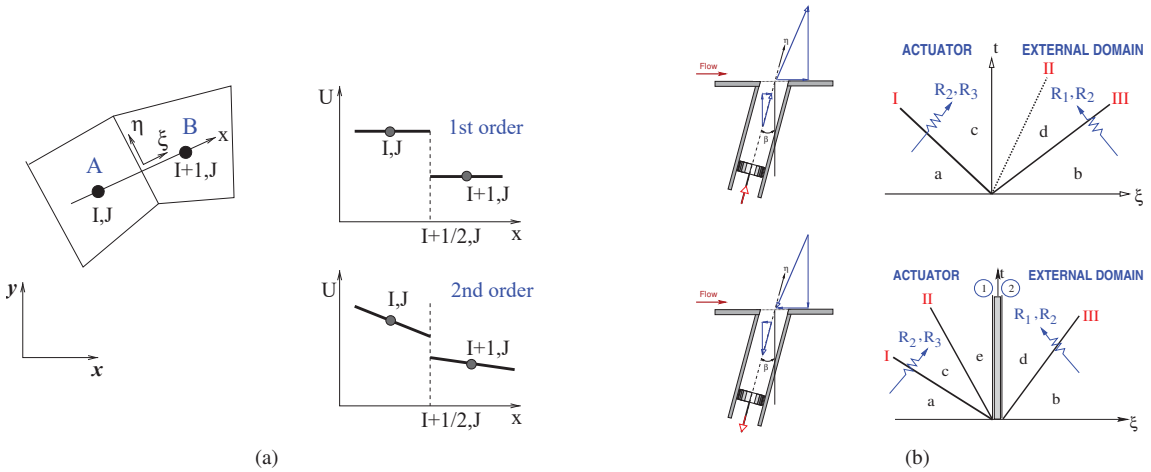

FIGURE 1. Evaluation of Fluxes: (a) Riemann problem at inner cell interfaces; (b) wave pattern of the Riemann problem at the SJ exit for the blowing *(top)* and suction phase *(bottom)*.

MATHEMATICAL MODEL

The flow governing are the compressible Unsteady Reynolds Averaged Navier-Stokes equations (RANS) written in the compact integral form

$$\frac{\partial}{\partial t}\int_{\mathcal{V}} \vec{W} d\mathcal{V} + \int_{\mathcal{S}} \vec{F}_I \cdot \hat{n} d\mathcal{S} + \int_{\mathcal{S}} \vec{F}_V \cdot \hat{n} d\mathcal{S} = \int_{\mathcal{V}} \vec{H} d\mathcal{V} \tag{1}$$

in an arbitrary volume $\mathcal{V}$ enclosed in a surface $\mathcal{S}$. With usual conventions, $\vec{W} = \{\rho, \rho\vec{q}, E, \tilde{\nu}_t\}^T$ is the hyper-vector of conservative variables, $\vec{F}_I$ and $\vec{F}_V$ are tensors containing the inviscid and the viscous fluxes, respectively.

$$\vec{F}_I = \left\{\rho\vec{q}, p\bar{\bar{I}} + \rho\vec{q}\otimes\vec{q}, (E+p)\vec{q}, \tilde{\nu}_t\vec{q}\right\}^T, \qquad \vec{F}_V = \frac{\sqrt{\gamma M_\infty}}{\mathrm{Re}_\infty}\left\{0, -\bar{\bar{\tau}}, -\kappa\nabla T - \bar{\bar{\tau}}\cdot\vec{q}, -\frac{\nu+\tilde{\nu}_t}{\sigma}\nabla\tilde{\nu}_t\right\}^T \tag{2}$$

$\vec{q} = \{u, v, w\}^T$ is the velocity vector, E the total energy per unit volume, M_∞ and Re_∞ are the free-stream Mach number and the Reynolds number, γ is the ratio of the specific heats and $\bar{\bar{I}}$ is the unit matrix. The term $\vec{H}$

$$\vec{H} = \left\{0, 0, 0, c_{b1}\tilde{S}\tilde{\nu}_t + \frac{c_{b2}}{\sigma}(\nabla\tilde{\nu}_t)^2 - c_{w1}f_w\left(\frac{\tilde{\nu}_t}{d}\right)^2\right\}^T \tag{3}$$

contains turbulence model source terms. The viscous stresses are $\tau_{ij} = (\mu+\mu_t)\left[\frac{\partial q_j}{\partial x_i} + \frac{\partial q_i}{\partial x_j} - \frac{2}{3}(\nabla\cdot\vec{q})\delta_{ij}\right]$.

The laminar viscosity μ is computed via the Sutherland's law. The turbulent viscosity $\mu_t = \rho\nu_t$ is defined according to the Spalart-Allmaras (S-A) model. The reader is referred to Ref. [10] for the explanation of the S-A model.

The numerical solution of system (1) is based on a Godunov method using Flux-Difference Splitting and an Essentially Non-Oscillatory scheme second order accurate in both time and space. The integration in time is carried out according to a 4th order Runge Kutta scheme. The Boundary Condition (BC) enforcement follows the guidelines of the characteristic based approach[11]. The numerical details and code validation can be found in Ref. [8, 9]. The numerical method has been parallelized by using OpenMP. The numerical framework for the unsteady simulation of FTV in open and closed-loop conditions has been already validated for the case of continuous blowing [8, 9].

As an additional feature, the flow control by using synthetic jets (SJ) has been introduced. SJ actuators are often simulated by a rough sinusoidal forcing function expressed as a boundary condition on the velocity profile at the actuator exit. This approach does not preserve the hyperbolic nature of the Navier-Stokes equations and the nonlinear nature of the bidirectional interaction between main-flow and actuator. This inconsistency elads, for instance, to an inaccurate evaluation of the static pressure at the actuator exit. A reduced order model that overcomes this weakness has been formulated in Ref. [5] . By using domain decomposition, the flow inside the actuator is simulated by the

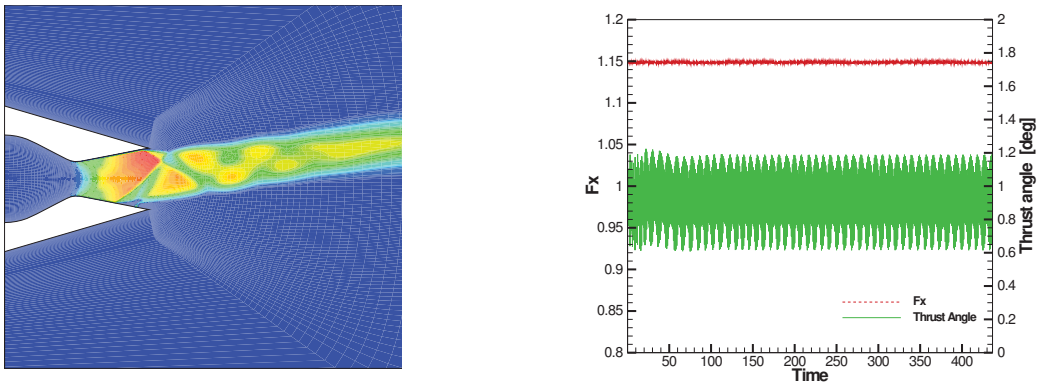

(a) (b)

FIGURE 2. Shock Vector control. (a) Flowfield on a jet-vectoring nozzle with steady blowing. (b) Response of the same nozzle in terms of axial force and thrust vector angle when steady blowing is replaced by a single SJ actuator.

unsteady 1-D compressible Euler equations, whereas the flow state at the interface between the two fields is evaluated by solving a Riemann problem between the internal and the external flow at each grid cell adjacent to the actuator orifice. The suction phase and the blowing phase are treated separately in order to comply with the hyperbolic nature of the flow equations. The corresponding wave patterns are represented in Figure 1b. The flow governing equations are integrated using a finite volume method fully compliant to that used for the external flow and having the same accuracy properties [5] .

NUMERICAL RESULTS

The Shock Vector approach to thrust vectoring uses a secondary steady blowing near the nozzle exit to generate an oblique shock that induces the side loads. A typical example of the computed nozzle flowfield with steady blowing computed is shown in Figure 2(a). Preliminary results obtained by using a single SJ actuator did not show a comparable effectiveness with respect to the steady blowing. Under the prescribed SJ forcing, the thrust angle remains very low, with a mean value of about one degree, as shown in Figure 2(b). Deeper investigations will be carried out.

The Dual-Throat Nozzle (DTN) concept of Figure 3a is a 2-D convergent-divergent-convergent nozzle with two geometric minimum areas and a cavity formed by these areas. The injection slot is located at the upstream minimum area. As visible in Figure 3c, the one-side injection of secondary flow creates an asymmetric pattern in the main stream. The secondary blowing forces the flow to separate in the cavity located on the injection side. The sonic plane becomes skewed, thus vectoring the primary flow [2].

The DTN system is better suited for SJ control. In fact, the induced separation and the generation of vortex flows in the cavity plays a major role in this jet-vectoring mechanism. As observed in many vortical flows [12] a weak forcing, as in the SJ case, can lead the system to very different vortex pattern. In a set of numerical experiments, we replaced the injection slot by one or more SJ actuators located close to the first throat. The nozzle response to the forcing of two actuators is presented in Figure 3d . As visible, remarkable vectoring effects can be produced. In present case the thrust vector angle δ is about 6 degrees. Thrust angles close to the steady blowing case ($\delta \simeq 12^o$) has been also obtained by varying the forcing frequency, the phase displacement, the SJ location and number.

CONCLUSIONS

A computational tool for the investigation of FTV strategy has been presented. FTV applies active flow control strategies on fixed nozzle in order to realize jet-vectoring effects normally obtained by deflecting a movable nozzle. The

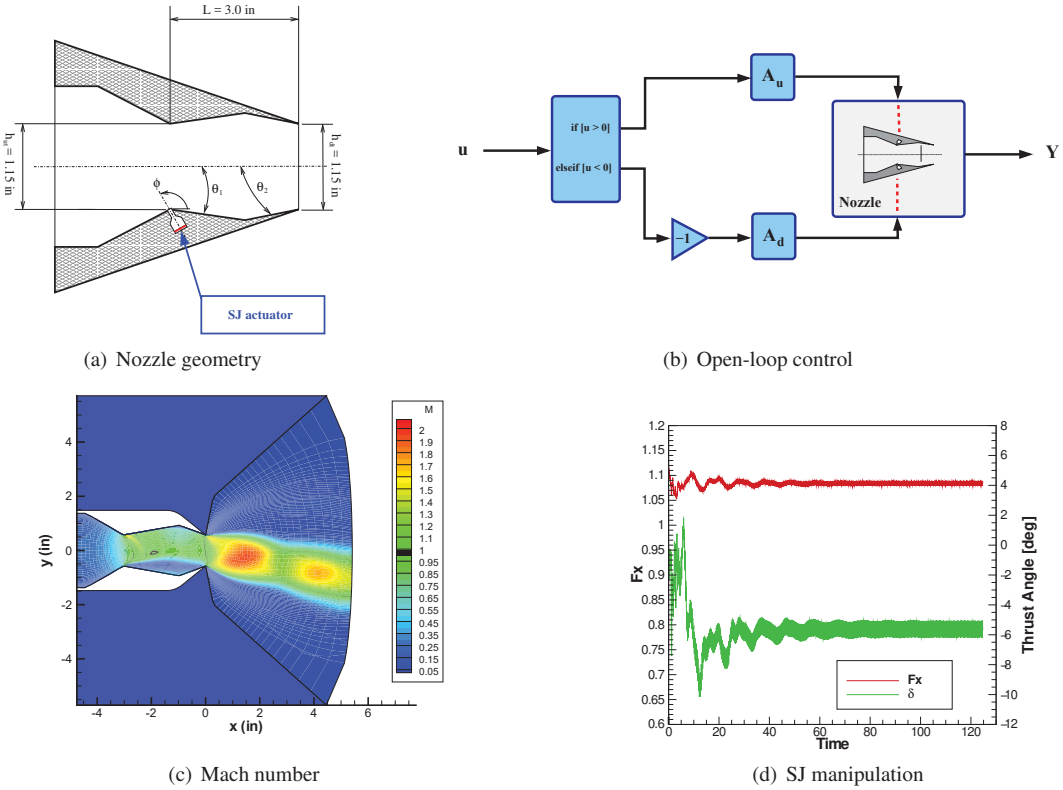

(a) Nozzle geometry

(b) Open-loop control

(c) Mach number

(d) SJ manipulation

FIGURE 3. Jet-vectoring of a Dual-Throat Nozzle. (a) Nozzle geometry and (b) control system; (c) flow field on a deflected condition by continuous blowing ($\delta = 12^o$) and (d) nozzle response to the control by two SJ actuators placed near the first throat.

numerical method has been validated for the continuous blowing of the supersonic DTN tested at NASA LaRC, [2, 8, 9]. In present work the numerical tool has been extended to include SJ manipulators and both techniques have been applied successfully to two nozzle configurations, e.g. DTN and shock vector control.

ACKNOWLEDGMENTS

Computational resources were provided by hpc@polito.it, a project of Academic Computing within the Department of Control and Computer Engineering at the Politecnico di Torino (http://www.hpc.polito.it).

REFERENCES

[1] S. Asbury and F. Capone, J. of Prop. Pow. **10** (1994).
[2] K. Deere, 21st AIAA Appl. Aerodyn. Conf., AIAA-2003-3800 (2003).
[3] P. Yagle, D. Miller, K. Ginn, and J. Hamstra, ASME J. of Eng. for Gas Turb. and Pow. **123**, 502–507 (2001).
[4] K. Deere, J. Flamm, B. Berrier, and S. Johnson, 43rd AIAA Joint Prop. Conf., AIAA 2007-5085 (2007).
[5] M. Ferlauto and R. Marsilio, Adv. in Aircr. and Spacecr. Sci. **2**, 77–94 (2014).
[6] D. Guo, A. Cary, and R. Agarwal, AIAA Journal **41** (2003).
[7] D. Gonzalez, D. Gaitonde, and M. Lewis, Int. Journal of Computational Fluid Dynamics **29**, 240–256 (2015).
[8] M. Ferlauto and R. Marsilio, Adv. in Aircr. and Spacecr. Sci. **3**, 367–378 (2016).
[9] M. Ferlauto and R. Marsilio, AIAA J. **55**, 86–98 (2017).
[10] P. Spalart, F. Johnson, and S. Allmaras, 7th Int. Conf. on Comput. Fluid Dyn., ICCFD7-1902 1–11 (2012).
[11] T. Poinsot and S. Lele, J. Comp. Phys. **101**, 104–129 (1992).
[12] A. Elcrat, M. Ferlauto, and L. Zannetti, Fluid Dyn. Res. **46**, p. 031407 (2014).